Formation Mechanism of a Periodic Nanograting Structure by a Surface Plasma Wave*)

Amany Moustafa GOUDA, Hitoshi SAKAGAMI[1)], Tomoya OGATA, Masaki HASHIDA[2)] and Shuji SAKABE[2)]

Department of Physics, Nagoya University, Nagoya 464-8602, Japan
[1)]*National Institute for Fusion Science, Toki, Gifu 509-5292, Japan*
[2)]*Institute for Chemical Research, Kyoto University, Gokasho, Uji, Kyoto 611-0011, Japan*

(Received 30 November 2015 / Accepted 4 February 2016)

A two-dimensional particle in cell code has been used to demonstrate the formation mechanism of a periodic nanograting structure in the hydrogen plasma. By using a linearly polarized, ultrafast laser beam with a wavelength of 800 nm, an incidence angle of 0°, and an intensity of 10^{16} W/cm^2–μm^2, the periodic nanograting structure was clearly self-organized at the boundary between a preformed and dense plasma at $t = 600$ fs. The bidirectional surface plasma wave plays a significant role together with the oscillating two-stream instability in producing the periodic nanograting structure.

Keywords: periodic nanograting structure, laser, plasma, laser plasma interaction, surface plasma wave, ponderomotive force, oscillating two-stream instability

DOI: 10.1585/pfr.11.2401071

1. Introduction

The production of a periodic nanograting structure by using an ultrafast laser beam is considered one of the most important techniques used to produce materials in the nanoscale. Periodic nanograting structures that are self-organized on the surface of solid materials such as insulators [1–3], semiconductors [4], and metals [5, 6] produced by irradiating with ultrafast laser pulses have been reported since 1999. These structures were oriented perpendicular or parallel to the direction of the laser polarization. Periodic nanograting structures have been used in numerous engineering fields for metal coloring [7, 8], in chemistry for protein folding [9], and in several other areas. For laser fluence levels just above the ablation threshold, the periodic nanograting structures have an interspace of 0.1 λ_L to 0.9 λ_L, which is shorter than the laser wavelength λ_L. The interspaces of the periodic nanograting structures depend on the laser fluence and wavelength. The phenomena of the periodic nanograting structure has been explained by different models, such as the parametric decay model [10], the plasmon polariton excitation model [11], and the second harmonic generation model [12]. However, the mechanism of the periodic structures is still under debate and additional investigations are needed. This paper analyzes one of the formation mechanisms for producing the periodic nanograting structure in the simulation framework.

2. Simulation Framework Details

In a similar manner to the experimental framework reported in [13], our simulation framework was divided into two regions. The first region is called mimic (preformed) plasma, and it represents the first plasma produced in the experimental study. It has a low electron density with an assumed value n_{mimic} of 0.7 n_{cr}, where n_{cr} is the critical density. The mimic plasma expands on the x-axis in the range of 0 to 2 μm and on the y-axis in the range of −3.6 to 3.6 μm. The second region is called (dense) target plasma, and it lies behind the mimic plasma. It has a high electron density with an assumed value n_{target} of 10 n_{cr} and expands on the x-axis in the range of 2 to12 μm and on the y-axis in the range of −3.6 to 3.6 μm. The ultrafast laser light with intensity $I = 1.0 \times 10^{16}$ W/cm^2–μm^2, λ_L = 800 nm and rise time = 15 fs is continuously irradiated onto the target at normal incidence (Fig. 1). In our simulation framework, the hydrogen plasma was characterized by the electron temperature (T_e) of 1 keV, ion temperature (T_i) of 0.1 keV, and a mass ratio (M_i/m_e) of 1836/16, where M_i and m_e are the ion and electron mass, respectively. This mass ratio value aims at reducing the calculation time. The particle in cell code (PIC) FISCOF2 was used to study the formation mechanism [14].

In the experimental framework (3D), the periodic nanograting structure is always parallel to the electric field component of the laser beam. In contrast, in the simulation framework (2D), we must choose a p-polarized laser beam to form a periodic nanograting structure that is parallel to the polarization direction. In the case of the s-polarized laser beam, the periodic nanograting structure cannot be

author's e-mail: amany.gouda@nifs.ac.jp
*) This article is based on the presentation at the 25th International Toki Conference (ITC25).

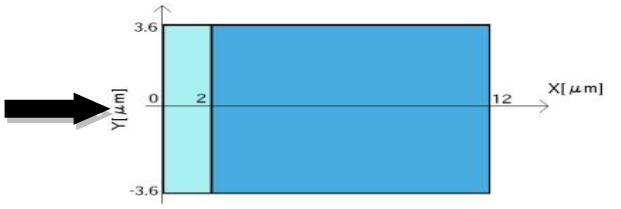

Fig. 1 Schematic for the simulation framework, showing the target plasma with the dimensions x = 2 - 12 μm, y = −3.6 - 3.6 μm, and density n_{target} = 10 n_{cr} and mimic plasma with the dimensions x = 0 - 2 μm, y = −3.6 - 3.6 μm and density n_{mimic} = 0.7 n_{cr}.

formed.

3. Simulation Results and Discussion

The formation mechanism of the periodic nanograting structure produced by using an ultrafast laser beam can be explained through a series of phenomena, beginning with the surface plasma wave formation and ending with the effect of the oscillating two-stream instability in the target plasma. The periodic nanograting structure is clearly shown in the simulation result of the electron density profile (Fig. 2). The electron density profiles show the formation of the periodic nanograting structure with the time evolution t = 400, 500, and 600 fs. We can estimate the interspace size average from the electron density profile of t = 400, 500, and 600 fs, which is about 0.2, 0.4, and 0.6 λ_L, respectively. The interspace size was found to be compatible with that of the experimental result [15]; also, the interspaces size increase with increasing the electron density n_e. In addition, Fig. 2 shows that the periodic nanograting structure was formed in an intermediate area found between the mimic and target plasmas. The intermediate area is formed when the laser energy is absorbed by the target plasma and the electron temperature increases; the target plasma expands by the sound velocity and the intermediate area will be formed. We note that as the electron density increases, the intermediate area slowly increases with time. See the color scale bar in Fig. 2.

The formation of the periodic nanograting structure begins when the p-polarized laser beam is continuously irradiated onto the target plasma for a period of 0 to 1000 fs. A surface plasma wave is produced at the intermediate area at the interface of the mimic and intermediate plasma. The electric field component of the laser beam E_L, in the y-direction, excites the collective behavior of the electrons. The motion of the electrons in both directions, the positive and negative y-directions, excites the electric field of the surface plasma wave that propagates near the surface and forms a standing wave. With satisfying the boundary condition of the surface plasma wave $\varepsilon_{low} \cdot \varepsilon_{High} < 0$ and $\varepsilon_{low} + \varepsilon_{high} < 0$, where ε_{high} and ε_{low} are the dielectric constants of the intermediate area plasma and the mimic plasma, the surface plasma wave will be formed. The formation and properties of the surface plasma wave

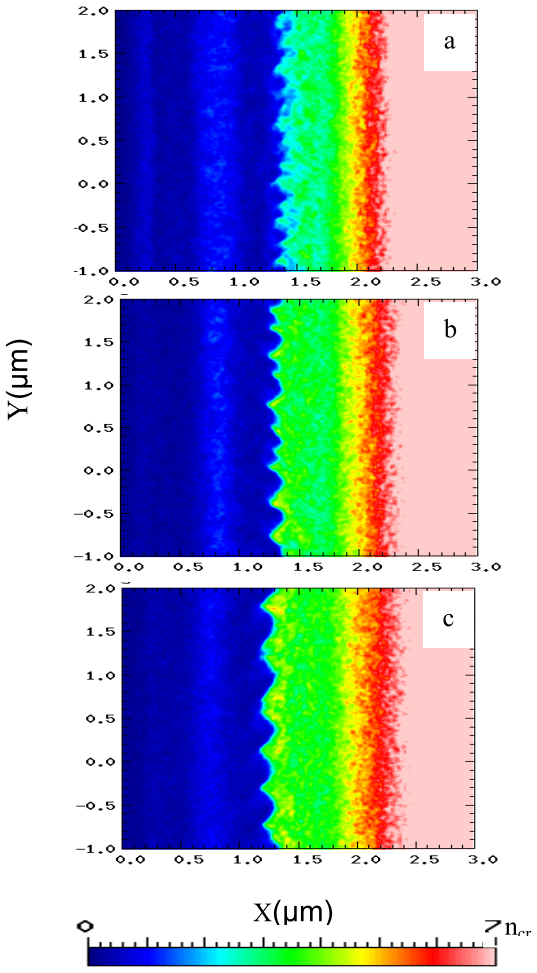

Fig. 2 Simulation results for the electron density profile in the x–y plane; snapshots at (a) t = 400 fs, (b) t = 500 fs, and (c) = 600 fs. The density profile shows the formation of the periodic nanograting structure with time evolution.

have been studied extensively in previous studies [16–18]. Eq. (1) describes the dispersion equation of the surface plasma wave as a function of the dielectric constants ε_{high} and ε_{low}. The dielectric constant of the mimic plasma ε_{low} will be considered as a vacuum and equals 1 due to the laser beam effect. The terms ω_{sp} and ω_{pe} are the surface plasma wave frequency and plasma frequency, respectively. The term k_{sp} is the wavenumber of the surface plasma wave. In the case of $\omega_{sp} = \omega_L$, it is found that wavelength of the surface plasma wave λ_{sp} increases with increasing electron density n_e, in the intermediate area (See Eqn. (2) and Fig. 2) depending on the electron density (n_h, n_L) of the intermediate and mimic plasma respectively. The dispersion relation diagram of the surface plasma wave at different values of n_e is shown in Fig. 3. It was found that k_{sp}/k_L decreases with increasing n_e.

$$k_{sp} = \frac{\omega_{sp}}{c}\sqrt{\frac{\varepsilon_{high} \cdot \varepsilon_{low}}{\varepsilon_{high} + \varepsilon_{low}}}$$
$$\varepsilon = 1 - \frac{\omega_{pe}^2}{\omega_{sp}^2} = 1 - \frac{n_e}{n_{cr}}, \quad (1)$$

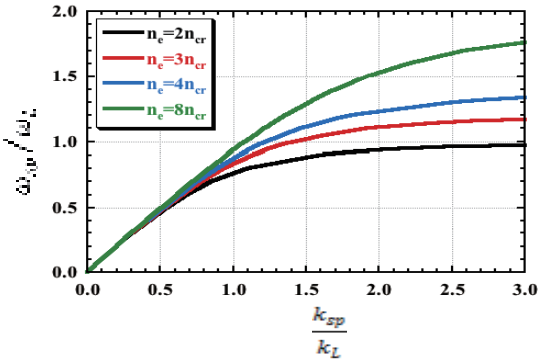

Fig. 3 Dispersion relation diagram for the surface plasma wave. The diagram shows the surface plasma wavenumber decreasing with increasing electron density.

At; $\omega_L = \omega_{sp}$

$$\frac{\lambda_{sp}}{\lambda_L} = \sqrt{\frac{2-\left(\frac{n_h + n_L}{n_{cr}}\right)}{\left(1-\frac{n_h}{n_{cr}}\right)\left(1+\frac{n_h}{n_{cr}}\right)}}. \quad (2)$$

The ponderomotive forces of the standing wave lead to the formation of a series of small tips on the intermediate area between the mimic–intermediate plasmas. The tips act as seeds for the periodic nanograting structure. In the area of density perturbation (area with small tips), the oscillating two- stream instability is considered as the mechanism of growth enhancement for the periodic nanograting structure. Although the oscillating two-stream instability has been studied in many textbooks as a nonlinear phenomenon [19], we will introduce a brief description to explain its role in our formation mechanism. Let E_L be the electric field component of the laser beam on the y-axis. The electrons will move in the opposite direction to E_L, and the ions will be fixed. A charge separation will occur, and the electrostatic charges will create an internal electric field E_1, which will oscillate at a frequency ω_L. The ponderomotive force as a result of the total field E_L and E_1 will enhance the tips to form the periodic nanograting structure.

The ponderomotive force FNL is calculated from Eq. (3)

$$F_{NL} = -\frac{\varepsilon_o \omega_{pe}^2}{\omega_L^2} \nabla \frac{(E_L + E_1)^2}{2}. \quad (3)$$

F_N does not average to zero because E_1 changes sign with E_L all the time. The ponderomotive force F_{NL} equals zero at the peaks and valleys of the charge density wave, whereas F_{NL} is large when ∇n_e is large. The spatial distribution causes F_{NL} to push electrons from regions of low density to regions of high density. With the motion of the electrons from one region to another, a (dc) electric field is produced and drags the ions, so the density perturbation increases. There is natural pressure $n_e(kT_e + kT_i)$ leading to the removal of the density perturbation; however, F_{NL} is high enough to overcome that pressure, and as the density ripple does not propagate and as the real value of the density frequency equals zero, these are known as the oscillating two-stream instability. The periodic nanograting structure is then formed under the effect of the oscillating two-stream instability.

Eq. (4) shows the oscillating two-stream instability growth rate, γ_{ots}. The growth rate is an important factor for describing the growth of the oscillating two-stream instability. In our case, γ_{ots} is large enough so the oscillating two-stream instability can be grown and sufficiently recorded within our simulation time.

$$\frac{\gamma_{ots}}{\omega_t} = \alpha_o \cdot \frac{\lambda_L}{\lambda_{sp}} \sqrt{\frac{1}{2} \cdot \frac{m_e}{M_i} \cdot \frac{1}{\frac{n_e}{n_{cr}} - 1}} \quad (4)$$

$$a_o = 0.85\, \lambda_L \cdot \sqrt{I_L\,[10^{18}\,\mathrm{W/cm^2}]}.$$

4. Conclusion

The formation mechanism of the periodic nanograting structures was studied by the 2D PIC code using an ultrafast laser pulse with a high intensity (10^{16} W/cm^2–μm^2). The surface plasma wave and the oscillating two-stream instability played a significant role in explaining the formation mechanism. The periodic nanograting structure was observed with time enhancement for the electron density profile. At t = 600 fs, there were clear periodic nanograting structures with an interspace size of 0.6 λ_L that were formed at the interface of the mimic–intermediate area. The interspace sizes were found to be compatible with that of the experimental results.

[1] D. Ashkenasi, A. Rosenfeld, H. Varel, M. Wahmer and E.E.B. Campbell, Appl. Surf. Sci. **120**, 65 (1997).
[2] A.M. Ozkan, A.P. Malshe, T.A. Railkar and W.D. Brown, Appl. Phys. Lett. **75**, 3716 (1999).
[3] J. Reif, F. Costache, M. Henyk and S.V. Pandelov, Appl. Surf. Sci. **891**, 197 (2002).
[4] N. Yasumaru, K. Miyazaki, J. Kiuchi and H. Magara, (3rd Asian Pacific Laser Symposium (APLS2002), Osaka, Japan, 2002, pp. 27–31.
[5] J. Bonse, H. Sturm, D. Schmidt and W. Kautek, Appl. Phys. A **71**, 657 (2000).
[6] M. Hashida, M. Fujita, Y. Izawa and A.F. Semerok, *Laser Precision Microfabrication*, ed. by I. Miyamoto *et al.*, Proceedings of SPIE **4830**, 452 (2002).
[7] S. Matsumoto, A. Yane, S. Nakashima, M. Hashida, M. Fujita, Y. Goto and S. Takahashi, J. Am. Chem. Soc. **129**, 3840 (2007).
[8] A. Vorobyev and C. Guo, Laser Photonics Rev. **7**, 385 (2013).
[9] M. Kawamoto, M. Hashida, Y. Miyasaka, M. Shimizu *et al.*, IEEJpn., LAV-13-016, 7–10 (2013).
[10] S. Sakabe, M. Hashida, S. Tokita, S. Namba and K. Okamuro, Phys. Rev. B **79**, 033409 (2009).
[11] T. Itana, R. Torres, T. Sarnet and M. Sentis, J. Appl. Phys. **114**, 083104 (2013).
[12] T.Q. Jia, H.X. Chen, M. Huang, F.L. Zhao, J.R. Qiu, R.X. Li, Z.Z. Xu, X.K. He, J. Zhang and H. Kuroda, Phys. Rev.

B **72**, 125429 (2005).
[13] M. Hashida, L. Gemini, T. Nishii and Y. Miyasaka, Optical Society of America, paper **SF21.3** (2015).
[14] H. Sakagami and K. Mima, Proc. 2nd Int. Conf. on Inertial Fusion Sciences and Applications, Kyoto, 2001, Elsevier, Paris, pp. 380–383 (2001).
[15] S. Sakabe, M. Hashida, S. Tokita, S. Namba and K. Okamuro, Phys. Rev. B **79**, 033409 (2009).
[16] A. Bouhelier, F. Ignatovich, A. Bruyant and C. Huang, Opt. Lett. **32**, 17 (2007).
[17] J.M. Pitarke, V.M. Silkin and E.V. Chulkov, Rep. Prog. Phys. **70**, 1 (2007).
[18] J. Homola, S. Yee and G. Gauglitz, Sens. Actuators B, Chem. **54**, 3 (1999).
[19] F.F. Chen, Library of Congress Cataloging in Publication Data (Plenum Press, New York and London, 1974) p.362.